

# Fabrication of a ZnO piezoelectric micro cantilever with a high-aspect-ratio nano tip

S. H. Lee, S. S. Lee, J.-J. Choi, J. U. Jeon, K. Ro

416

**Abstract** This paper reports on a ZnO piezoelectric micro cantilever with a high-aspect-ratio (HAR) nano tip, which is proposed for a ferroelectric material based nano storage system. The system uses the interaction between the nano tip and a storage medium, and the HAR nano tip is needed to suppress undesirable effects caused by the small gap between the cantilever and the storage medium. The fabrication process for the cantilever with the HAR nano tip consists of three parts: the HAR nano tip formation, the cantilever fabrication, and the bonding/releasing process. The HAR nano tip is formed by the Si deep reactive ion etching for a long shaft and the anisotropic wet etching for a nano tip end. The cantilever is made up of 1  $\mu\text{m}$ -thick LPCVD poly-Si layer and 0.2  $\mu\text{m}$ -thick Si nitride layer, and has 0.5  $\mu\text{m}$ -thick ZnO actuation layer. A final releasing process is followed by an anodic bonding process. The fabricated HAR nano tip has 6  $\mu\text{m}$  side length, over 18  $\mu\text{m}$  height, and less than 15 nm tip radius, which is built on the 85  $\mu\text{m}$ -wide, 300  $\mu\text{m}$ -long, and 1.2  $\mu\text{m}$ -thick cantilever. The experimental results show a linear behavior with respect to input voltage of 1 to 5 V and the first resonance frequency at 17.9 kHz.

## 1 Introduction

The bit areal density of a commercial magnetic disk drive has been increased with a compound annual growth rate of 60%, driven by the development of technologies like new fabrication techniques of a hard disk head and high precision actuator control techniques [1]. However, despite of the rapidly advancing technologies, it is expected that magnetic storage cannot be used for storage with capacities exceeding 100–200 Gb/in<sup>2</sup> in areal density because of the superparamagnetic limit [1, 2].

The development of a scanning probe microscopy (SPM) and new materials for storage media give the vision to overcome the superparamagnetic limit and to achieve the tera or peta bit/in<sup>2</sup> areal density. Since the first development at early 80's, various kinds of the SPMs have been proposed, such as a scanning tunneling microscopy (STM), an atomic force microscopy (AFM), a magnetic force microscopy (MFM), and a scanning near-field optical microscopy (SNOM) [3]. Many researchers have applied them to the future nano storage systems using polymers, dielectric and ferroelectric materials as the storage media [4–6].

Compared with other nano storage systems, the system of the AFM with a non-volatile ferroelectric material like PZT has several advantages; it is easy to read, write, and rewrite with the electrical signal and has high recording density and fast switching time [6–9]. Since Franke et al. modified and detected the polarized ferroelectric domains on PZT films using a conductive AFM tip at 1994 [8], a lot of researches have shown that the ferroelectric film has the potential for the AFM based recording media [6–10].

While the AFM is performing the data storage operation, the electrostatic interaction between the nano tip and the ferroelectric medium is the major contributing factor for domain contrast. However, the usage of short AFM tips may lead to critical shortcoming because of the interaction between the AFM cantilever and the storage medium [10]. Therefore, the cantilever needs to have the HAR nano tip for enhanced reading and writing operations.

In addition, the cantilever is also required to integrate an actuator for following the topographic feature of the storage medium and for achieving the high resonance frequency [11]. Many researches have been performed on the cantilevers with piezoelectric films such as PZT or ZnO films [11–13]. Although LG fabricated the cantilever array with PZT [13], the difficulty in the process of the PZT film is not completely solved due to the delicate chemical nature and the process of ZnO film can be more easily performed using the sputtering process.

Received: 20 October 2003 / Accepted: 27 August 2004

S. H. Lee (✉)  
Department of Mechanical Engineering,  
Pohang University of Science and Technology,  
San 31 Hyoja-dong Nam-gu, Pohang,  
Kyungbuk 790-784, Korea  
e-mail: hyla@postech.ac.kr

S. S. Lee  
Department of Mechanical Engineering,  
Korea Advanced Institute of Science and Technology,  
Daejeon 305-701, Korea

J.-J. Choi  
ICurie Lab Inc., Seoul 135-846, Korea

J. U. Jeon  
School of Mechanical and Automotive Engineering,  
University of Ulsan, Ulsan 680-749, Korea

K. Ro  
Samsung Advanced Institute of Technology,  
Yongin, Kyunggi 449-712, Korea

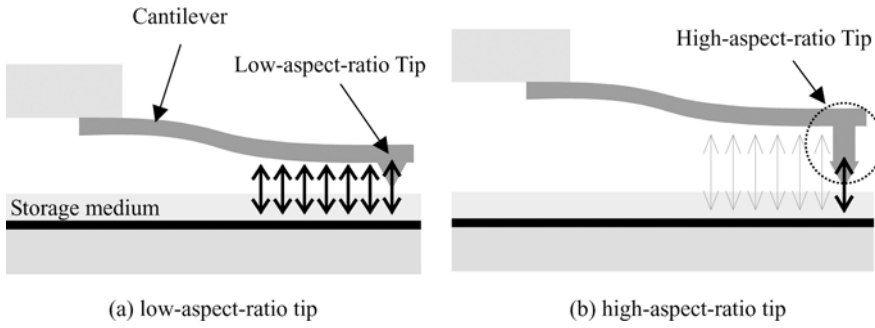


Fig. 1. Electrostatic interaction between cantilever and data storage medium

In this paper, we report the ZnO piezoelectric micro cantilever with a HAR nano tip. The HAR nano tip is designed and fabricated to reduce the inadequate effect, and the multi-layered structure is used to integrate the ZnO layer as the actuation layer. The feature of the HAR nano tip is examined, and the dynamic response of the cantilever is also investigated.

## 2 Device design

### 2.1 HAR nano tip

In a ferroelectric material based system, polarization is performed by the electrostatic interaction between the nano tip and storage medium. If the height of tip is not tall enough, the electrostatic interaction between the cantilever and the storage medium cannot be neglected compared with that between the tip and the medium as seen in Figure 1(a), which makes the domain contrast worse and affects on the reading process [10]. The interaction caused by the cantilever may affect storage material and distort stored data. The interaction force by the cantilever,  $F$  is given by

$$F = \frac{\partial E}{\partial d} = \frac{1}{2} V^2 \frac{\partial C}{\partial d} \quad \left( \text{where } C = \frac{\epsilon A}{d} \right) \quad (1)$$

where  $E$ ,  $V$ ,  $C$ ,  $\epsilon$ ,  $A$ , and  $d$  are the stored energy in capacitor, the applied voltage, the capacitance, the permittivity, the cantilever area, and the distance between the cantilever and the storage medium, respectively. Since  $F$  is inversely proportional to  $d^2$  as seen in Eq. (1), the undesirable effect of the cantilever with a HAR nano tip will be reduced as shown in Fig. 1(b).

### 2.2 Device and process design

Figure 2 shows the schematic overview of the ZnO piezoelectric micro cantilever with the HAR nano tip, which has 85  $\mu\text{m}$  width, 300  $\mu\text{m}$  length, and 1.2  $\mu\text{m}$  thickness. The pyrex glass is anodically bonded and supports the cantilever.

Figure 3a shows the formation process of the HAR nano tip. First, the Si deep reactive etching (DRIE) is used for the long shaft of the HAR nano tip (1). A thin thermal silicon oxide layer is grown to protect the sidewall (2). Using the blanket RIE, only the bottom silicon oxide layer of trench is removed due to the directionality of chemically active species and the silicon oxide thickness differ-

ence (3). After the nano tip end is formed with the anisotropic wet etching (4), the thermal oxidation is performed for the tip sharpening (5). The LPCVD poly-Si layer constitutes the HAR nano tip with the trench refilling process (6). In the conventional tip fabrication process [11–15], since a tip is fabricated in the early stage and it protrudes out of the plane, there is some problem in subsequent processes as shown in Fig. 3 b. In contrast, this trench refilling process can make the HAR nano tip buried in the trench and the top surface flat. Therefore, it makes the remaining processes easier compare to the conventional tip process. Moreover since the HAR nano tip is buried inside the trench till the releasing process, the HAR nano tip is protected during the whole process. It minimizes tip damage and results in high yield. It is also cost effective unlike the most previous SPM process using SOI wafers. [11–15].

The cantilever is composed of several layers: two poly-Si layers, a silicon nitride layer, a silicon oxide layer, a ZnO layer, and a Cr/Au layer as shown in Fig. 4. The first poly-Si layer is for the cantilever structure, and the second poly-Si layer works as the lower electrode and bonding pad in the anodic bonding process. The silicon nitride layer electrically separates two poly-Si layers, and prevents the direct contact of the lower electrode with pyrex glass during the anodic bonding process. The PECVD silicon oxide layer is used for the low frequency application of the

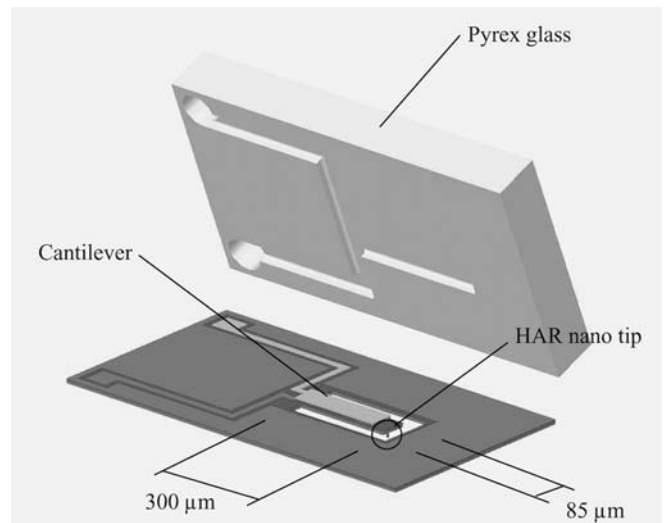
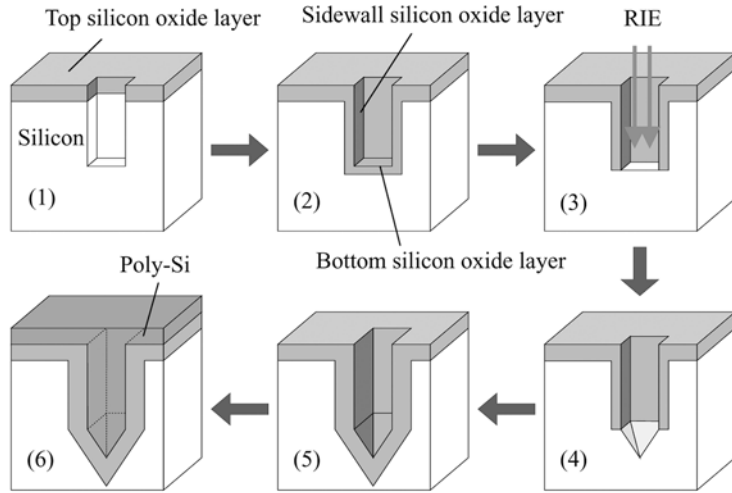
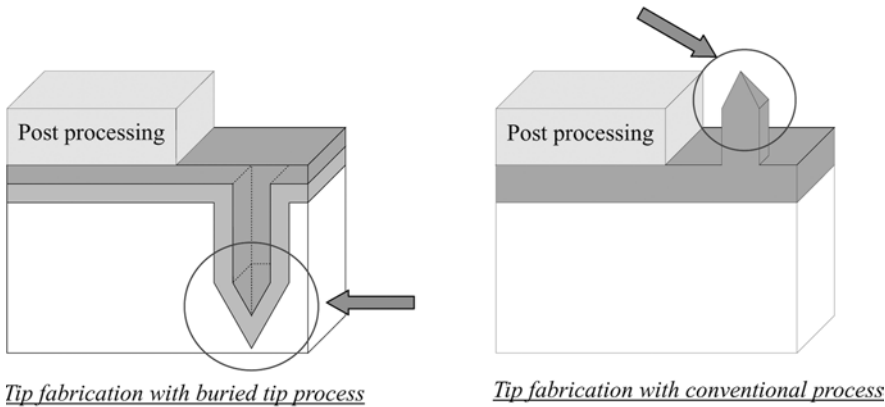


Fig. 2. Schematic and cross-sectional view of the cantilever with the HAR nano tip



(a) fabrication process for the HAR nano tip



(b) comparison of two methods to fabricate the HAR nano tip

Fig. 3. Fabrication process for the HAR nano tip

ZnO layer [16]. It also prevents short circuiting between the upper and the lower electrodes. The 0.03/0.3  $\mu\text{m}$ -thick Cr/Au layer is selected as the upper electrode and it protects the ZnO layer from BHF during the releasing process.

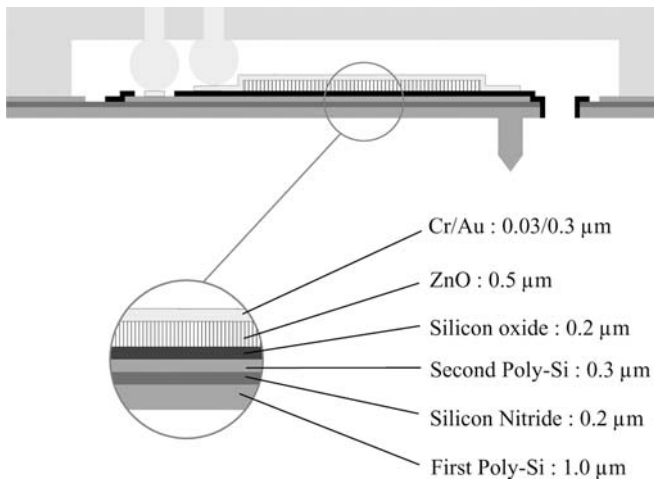


Fig. 4. Cross-sectional view of the cantilever with the HAR nano tip

The designed cantilever has a rectangular shape and has the dimension of 85  $\mu\text{m}$  width, 300  $\mu\text{m}$  length, and 1.2  $\mu\text{m}$  thickness. Since the device has multiple layers, the equivalent width and the cantilever deflection theory are applied for the calculation of the spring constant, and the value of 1.4 N/m is represented [17]. A resonance frequency is investigated using the FEM simulation tool, ABAQUS, and the first resonance frequency is found at 27.81 kHz as shown in Fig. 5.

### 3 Fabrication process

Figure 6 shows the detailed fabrication process, which consists of three parts: the HAR nano tip formation, the cantilever fabrication, and the bonding/releasing process. The HAR nano tip formation process starts with (100)-oriented Si wafers covered with a 0.7  $\mu\text{m}$ -thick thermal silicon oxide layer. After defining tip patterns, 12  $\mu\text{m}$ -deep trenches are etched with Si DRIE process. To protect the sidewall, a 0.2  $\mu\text{m}$ -thick thermal silicon oxide layer is grown. After etching of the bottom silicon oxide layer using the anisotropy of RIE, the pyramidal shaped tip is formed in a TMAH solution at 70  $^{\circ}\text{C}$ . For tip sharpening,

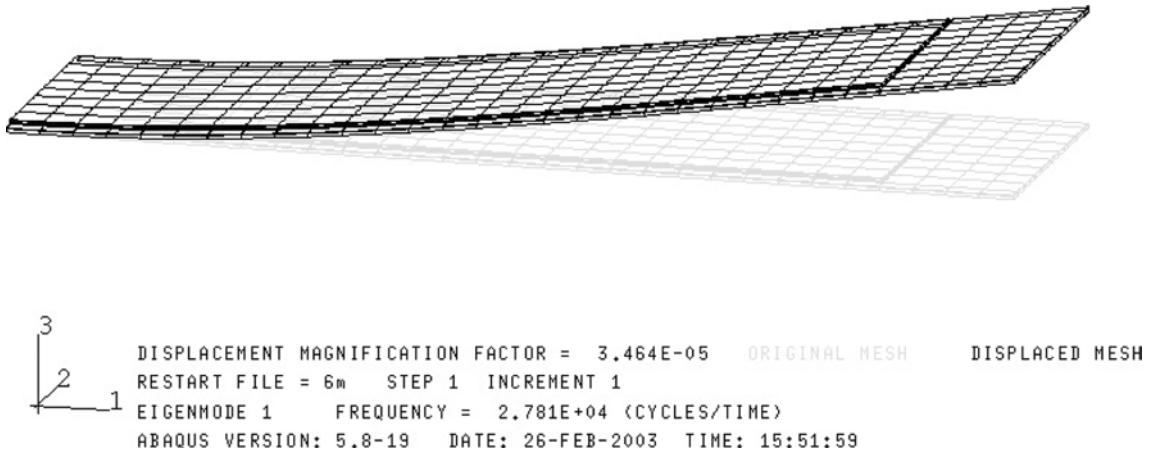


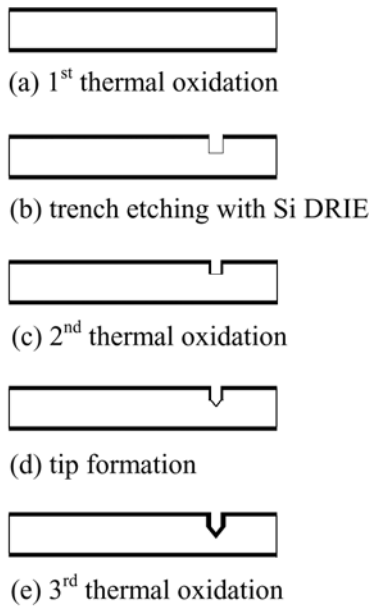
Fig. 5. A FEM simulation result of the cantilever

an over 1  $\mu\text{m}$ -thick thermal silicon oxide layer is grown at 1050  $^{\circ}\text{C}$ .

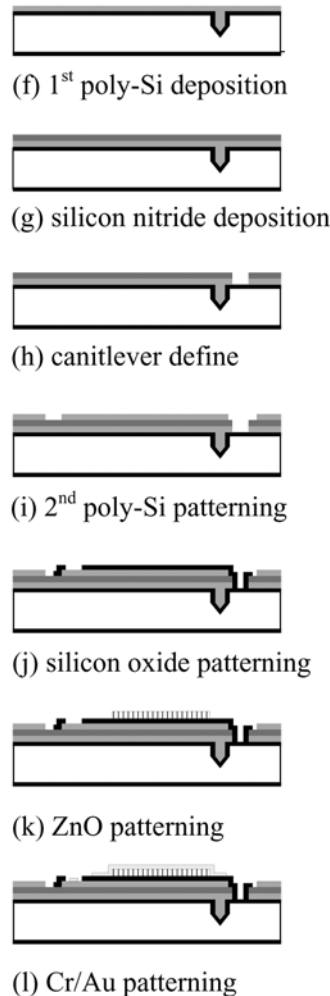
For the cantilever structure, a 1  $\mu\text{m}$ -thick LPCVD poly-Si layer is deposited. It also fills deep trenches and forms

the HAR nano tip. For the conductivity, phosphorous is diffused by pre-deposition at 900 $^{\circ}$  C for 15 minutes, followed by drive-in at 900  $^{\circ}\text{C}$  for 30 minutes in wet ambience. Another 0.3  $\mu\text{m}$ -thick LPCVD poly-Si electrode

***HAR nano tip formation***



***Cantilever fabrication***



***Bonding/releasing process***

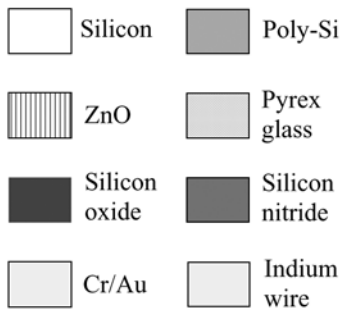
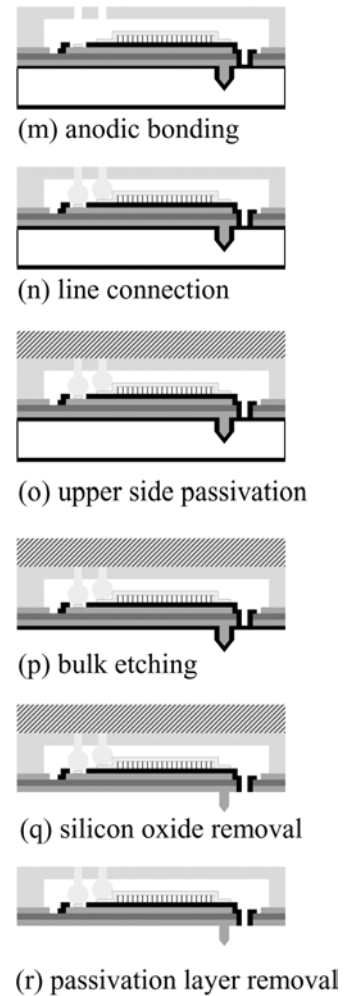


Fig. 6. Fabrication process flow

is formed over a 0.2  $\mu\text{m}$ -thick silicon nitride layer ( $\text{Si}_3\text{N}_4$ ). The second poly-Si layer is used for the lower electrode and the bonding layer. The silicon nitride layer isolates the poly-Si layer from the lower electrode and prevents the direct contact of the lower and upper electrodes with pyrex glass. A 0.5  $\mu\text{m}$ -thick ZnO layer is RF-magnetron sputtered onto a PECVD silicon oxide layer. The Cr/Au layer is deposited for the upper electrode with 30/300 nm thickness.

Anodic bonding process is performed to attach the second poly-Si layer to a supporting glass in the vacuum condition ( $1 \times 10^{-2}$  Torr), which prevents the oxidation of metal layers. Since pyrex glass doesn't establish contact with the upper and lower electrodes, it prevents ZnO breakdown during the bonding process. After the process, the inner electrodes are connected to the outer ones on the glass using an indium wire. After the upper side passivation of the glass, the Si substrate is removed using the TMAH solution and the Si DRIE. The silicon oxide layer which is used for tip sharpening protects the cantilever during the Si DRIE process. After removing the Si substrate, the silicon oxide layer is etched with BHF. The Cr/Au layer protects the ZnO layer during the releasing process. Finally, the device fabrication is completed after removing the upper side passivation layer.

The chief processing challenge of the process is to fabricate the HAR nano tip, and the Si DRIE and trench refilling process with the LPCVD poly-Si layer make it possible. This process protects the nano tip during the whole process and minimizes tip damages.

## 4 Results and discussions

### 4.1 Fabrication results

Figure 7 shows the device features during the fabrication process. Figure 7 (a) shows the monitoring tip patterns just after the nano tip etching with the TMAH, and the cross lines in the midpoint of squares represent final etched tip patterns. Figure 7 b shows the cantilever beam after ZnO patterning. Figure 7 c and d represent the cantilever after the anodic bonding process and the releasing process, respectively. During the anodic bonding process, the vacuum environment ( $1 \times 10^{-2}$  torr) prevents the oxidation of the Cr/Au layer. The separation of bonding parts from the electrodes prevents the ZnO breakdown. However, the cantilever bends downward because of residual stresses as seen in Fig. 7 d. All layers of the cantilever structure have the residual stresses: the ZnO layer, two poly-Si layers and the oxide layer have the compressive residual stresses and the nitride layer and the Cr/Au layer have the tensile residual stresses. The stress of each layer is affected with the process conditions, and the resulting stress varies from the designed values. The stress mismatch makes the cantilever bend downward.

Figure 8 represents SEM images of the fabricated cantilever with Philips XL30 S FEG-SEM. The height of the HAR nano tip is larger than 18  $\mu\text{m}$  as shown in the Fig. 8 b. The side length is 6  $\mu\text{m}$ , and the resulting aspect ratio is more than three. The corrugated sidewall features of the HAR nano tip is generated during the etching and

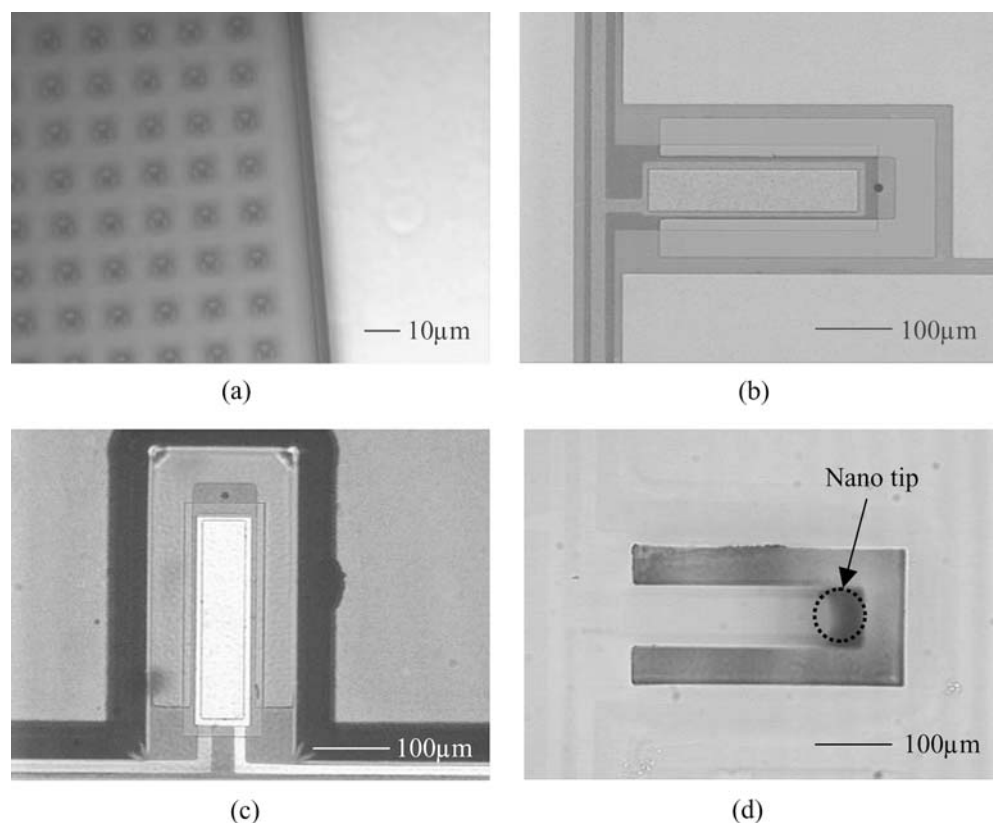
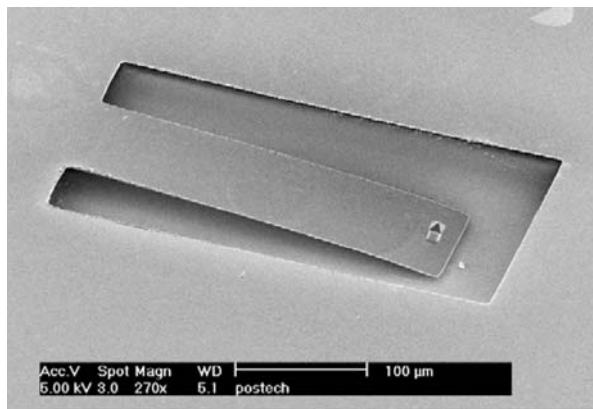
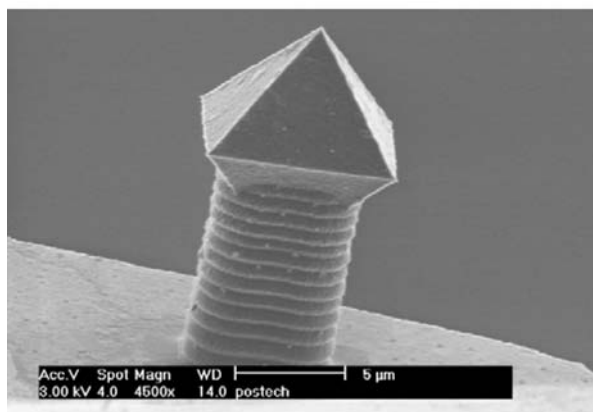


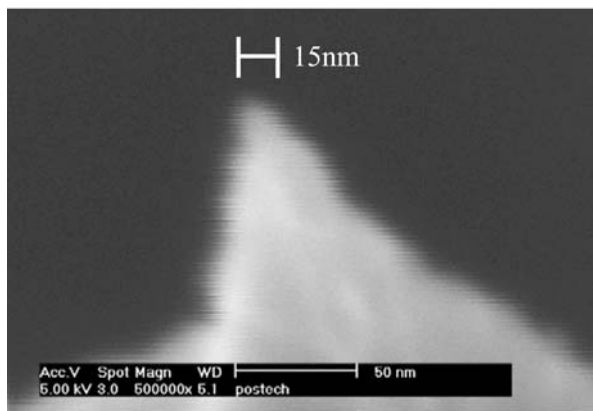
Fig. 7. Pictures of the cantilever during the fabrication process



(a) cantilever with HAR nano tip



(b) HAR nano tip



(c) enlarged view of a HAR nano tip

**Fig. 8.** SEM images of the fabricated cantilever with a HAR nano tip

passivation cycles of the Si DRIE process. Figure 8 c shows the sharp end of the HAR nano tip with less than 15 nm tip radius, which is not clear due to the limitation of environmental condition.

#### 4.2

##### Characteristics of the cantilever

The *c*-axis orientation of the ZnO layer is one of the most important factors of piezoelectric property, which is affected by the deposition conditions such as gas flow rate and substrate temperature. The X-ray diffraction (XRD)

pattern is used to investigate the *c*-axis properties at various conditions. In these cases, fixed working pressure and plasma power are applied which are 5 mtorr and 140 W, respectively. The resulting XRD graphs are shown in Fig. 9a. Some sharp peaks appear according to the crystal directions and the ratio of intensity of (002) peak with respect to those of other peaks must be large for the better *c*-axis property. Based on the peak ratio, the case 2 with the condition of 300 °C and 30/30 sccm Ar/O<sub>2</sub> flow rate represents the best result comparing to other cases. Moreover, the case 2 shows the sharp and large (002) peak, which indicates the ZnO layer has a *c*-axis normal orientation perpendicular to the substrate surface. Figure 9 b is the SEM image of sputtered ZnO layer at that condition and it also shows the *c*-axis orientation of the ZnO layer.

The resonance frequency is measured using the laser Doppler vibrometer (LDV, Polytec, OFV 511 and OFV 3001) and the dynamic signal analyzer (Stanford research system, SR785) as shown in Fig. 10 a. The LDV measures the frequency response by detecting the reflected laser beam from the sample surface. The sinusoidal 8 V<sub>p-p</sub> is applied during the measurement and the Fig. 10 b represents the response of the actuated cantilever. The measured first resonance frequency is 17.9 kHz, which is smaller than the simulated value. Figure 10c represents the static deflection of the cantilever with the variation of input voltage. It shows the linear behavior with respect to the input voltage up to 5 V.

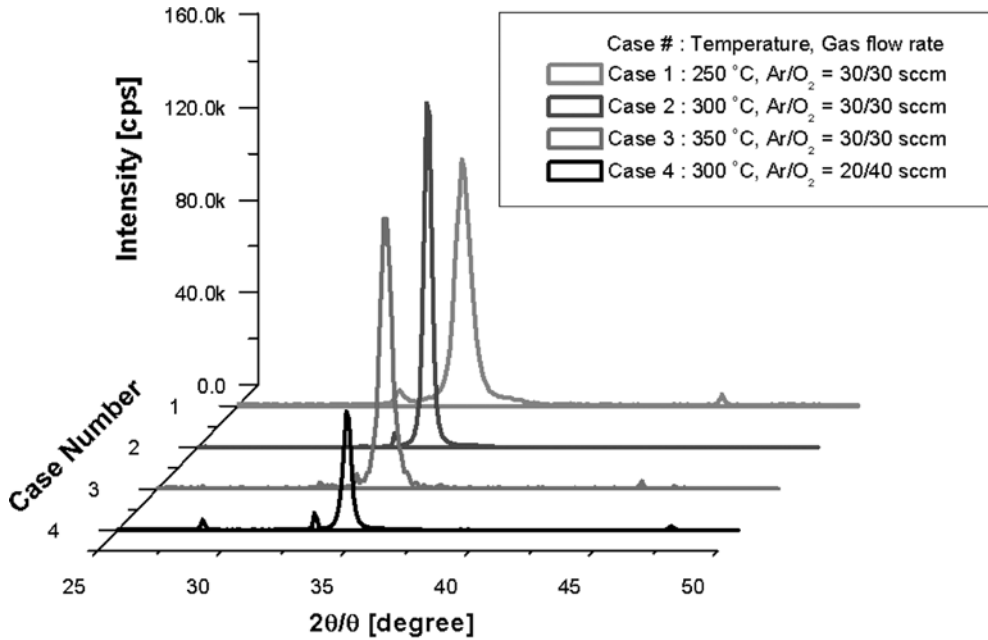
#### 5

##### Conclusions

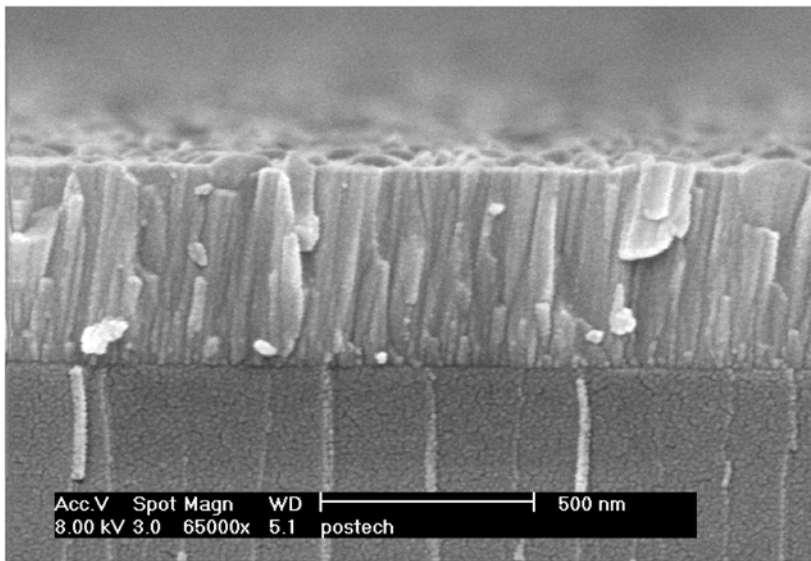
We designed and fabricated the ZnO piezoelectric cantilever with the HAR nano tip for a ferroelectric material based nano storage system. The cantilever with the HAR nano tip is fabricated by etching the trench with the Si DRIE and the tip end with the anisotropic wet etching, filling with the LPCVD poly-Si, and removing the Si substrate. It protects the nano tip during the whole processes and minimizes tip damage. The cantilever is supported by the anodic bonded pyrex glass and uses the ZnO layer as an actuation layer. The ZnO layer is deposited with the RF magnetron sputter, and the XRD pattern shows the well-established *c*-axis orientation of the ZnO layer. The multiple-layered structure prevents the direct contact of electrodes with the pyrex glass during the anodic bonding process, and it protects the breakdown of the ZnO layer. The vacuum condition prevents the oxidation of the upper electrode. The fabricated HAR nano tip integrated on the cantilever has 6 μm side length, over 18 μm height, and less than 15 nm tip radius. The enlarged gap between the cantilever and the storage medium by the HAR nano tip is expected to make the undesirable effect reduced. The frequency response is measured with the LDV and it shows the first resonance frequency of the cantilever at 17.9 kHz. The static deflection with respect to the input voltage represents the linear behavior up to 5 V.

##### References

1. Grochowski E; Hoyt RF (1996) Future trends in hard disk drives. IEEE Trans. Magn. 32(3): 1850-1854



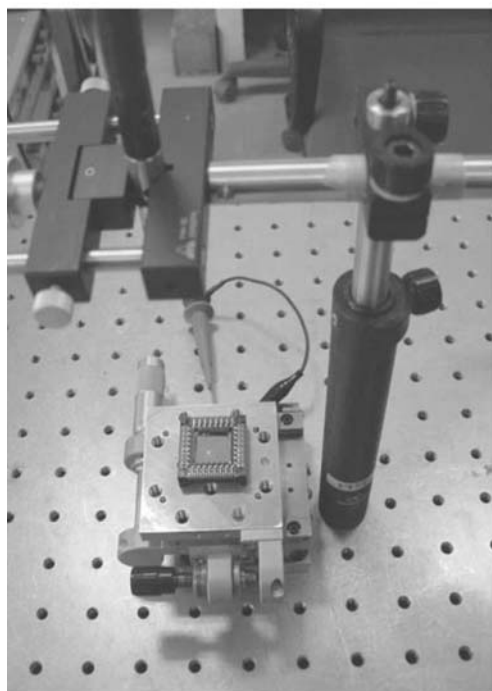
(a) X-ray diffraction patterns



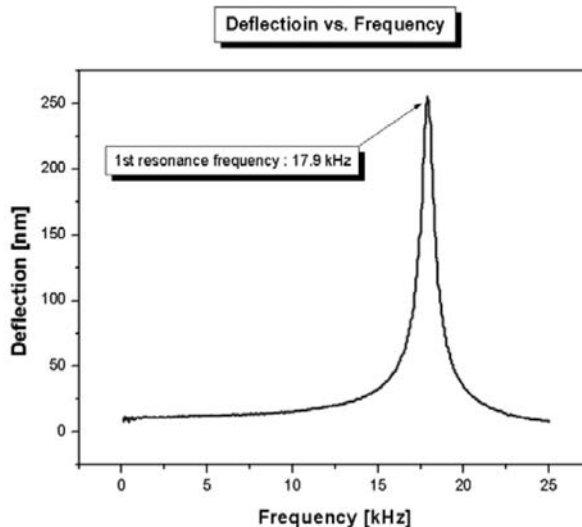
(b) SEM picture of the ZnO layer in case 2

Fig. 9. Characteristics of the sputtered ZnO layer under the various conditions

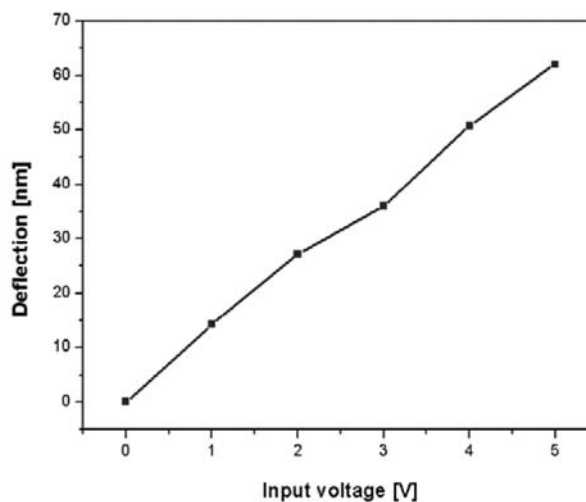
2. Thompson DA; Best JS (2000) The future of magnetic data storage technology. *IBM J. Res. Develop.* 44(3): 311–316
3. Wickramasinghe HK (2000) Progress in scanning probe microscopy. *Acta Mater.* 48(1): 347–358
4. Naberhuis S (2002) Probe-based recording technology. *J. Magn. Magn. Mater.* 249(3): 447–451
5. Hosaka S (2001) SPM based recording toward ultrahigh density recording with trillion bits/inch<sup>2</sup>. *IEEE Trans. Magn.* 37(2): 855–859
6. Shin H; Lee K; Moon W; Jeon JU; Pak YE; Park JH; Yoon KH (2000) An application of polarized domains in ferroelectric thin films using scanning probe microscope. *IEEE Trans. Ultrason., Ferroelect., Freq. Contr.* 47(4): 801–807
7. Ahn CH; Tybell T; Antognazza L; Char K; Hammond RH; Beasley MR; Fischer Ø; Triscone J-M (1997) Local, Nonvolatile Electronic Writing of Epitaxial Pb(Zr<sub>0.52</sub>Ti<sub>0.48</sub>)O<sub>3</sub>/SrRuO<sub>3</sub> Hetero-structures. *Science* 276: 1100–1103
8. Franke K; Besold J; Haessler W; Seegebarth C (1994) Modification and detection of domains on ferroelectric PZT films by scanning force microscopy. *Surface Science Letters* 302: L283–L288
9. Hidaka T; Maruyama T; Saitoh M; Mikoshiba N; Shimizu M; Shiosaki T; Wills KA; Hiskes R; Dicarolis SA; Amano J (1996) Formation and observation of 50 nm polarized domains in PbZr<sub>1-x</sub>Ti<sub>x</sub>O<sub>3</sub> thin film using scanning probe microscope. *Appl. Phys. Lett.* 68: 2358–2359
10. Hong S; Woo J; Shin H; Jeon JU; Pak YE; Colla EL; Setter N; Kim E; No K (2001) Principle of ferroelectric domain imaging using atomic force microscope. *J. App. Phys.* 89(2): 1377–1386
11. Manalis SR; Minne SC; Atalar A; Quate CF (1996) High-speed atomic force microscopy using an integrated actuator and optical lever detection. *Rev. Sci. Instrum.* 67(9): 3294–3297
12. Sulchek T; Minne SC; Adams JD; Fletcher DA; Atalar A; Quate CF (1999) Dual integrated actuators for extended range



(a) experimental setup  
: LDV (Laser Doppler Vibrometer) and  
dynamic signal analyzer



(b) dynamic response with respect to frequency



(c) static deflection with respect to input voltage

**Fig. 10.** Measurement of the static and the dynamic behaviors of the ZnO piezoelectric cantilever with HAR nano tip

- high speed atomic force microscopy. *Appl. Phys. Lett.* 75(11): 1637–1639
13. Kim Y; Nam H; Cho S; Hong J; Kim D; Bu JU (2003) PZT cantilever array integrated with piezoresistor sensor for high speed parallel operation of AFM. *Sens. Actuators A* 103(1–2): 122–129
  14. Vettiger P; Despont M; Drechsler U; Dürig U; Häberle W; Lutwyche MI; Rothuizen HE; Stutz R; Widmer R; Binnig GK (2000) The “Millipede”- More than one thousand tips for future AFM data storage. *IBM J. Res. Develop.* 44(3): 323–340
  15. Lutwyche M; Andreoli C; Binnig G; Brugger J; Drechsler U; Häberle W; Rohrer H; Rothuizen H; Vettiger P; Yaralioglu G; Quate C (1999)  $5 \times 5$  2D AFM cantilever arrays a first step towards a terabit storage device. *Sens. Actuators A* 73: 89–94
  16. Blom FR; Yntema DJ; van De Pol FCM; Elwenspoek M; Fluitman JHJ; Popma THJA (1990) Thin-film ZnO as micromechanical actuator at low frequencies. *Sens. Actuators A* 21–23: 226–228
  17. Lee SH; Lee SS; Choi J-J; Jeon JU; Ro K-C (2004) Fabrication of a high-aspect-ratio nano tip integrated micro cantilever with a ZnO piezoelectric actuator. *Key Engineering Materials* 270–273: 1095–1100